

## NOTES

## CO Hydrogenation over Well-Dispersed Carbon-Supported Iron Catalysts

Iron has long been the predominant Fischer-Tropsch catalyst for commercial use; however, significant improvements can still be made in the areas of selectivity and activity maintenance (1). Unsupported, promoted iron is the catalyst presently used, but few studies pertaining to supported iron have been reported, presumably because iron is so inexpensive. However, earlier studies indicated that using carbon as a support could alter catalytic behavior of metals like iron and ruthenium (2, 3). In addition, studies utilizing glassy carbons (carbon molecular sieves) showed that the ultramicroporosity in these carbons could affect selectivity in certain catalytic reactions (4). This led to an initial study focused on the preparation and catalytic behavior of iron/glassy carbon catalysts which has been described elsewhere (5-7). However, it rapidly became apparent that these carbon-supported iron systems were quite interesting and a broader base was required for comparison, so catalysts composed of iron dispersed on graphitized carbon, carbon blacks, and activated carbons were also prepared. In contradiction to earlier studies of Fe/carbon CO hydrogenation catalysts, these carbon-supported iron samples were very active, and they typically had higher activities and olefin/paraffin ratios than unpromoted Fe/Al<sub>2</sub>O<sub>3</sub> catalysts (5, 6).

In addition, an aqueous impregnation technique was developed which allowed the preparation of very highly dispersed iron on certain carbons. These iron/carbon catalysts could be placed in two general groups: one with high dispersion (HD) and one with low dispersion (LD). These reduced catalysts exhibited extremely interesting chemisorption behavior at 300 K—hydrogen chemisorption either did not

occur or was very low while CO chemisorption always occurred, with very large CO uptakes existing in some cases indicating the presence of very small iron particles (i.e., high dispersions) (5, 6). In addition to these chemisorption properties, significant differences existed in catalytic behavior which could be correlated with the crystallite size of the iron. This note describes these variations in catalytic properties.

The preparation of catalysts used in this work has been described previously (5, 6). For example, the two catalysts most thoroughly studied, 5% Fe/C-1 and 4.5% Fe/V3G, were prepared by wetting Carbolac-1 (C-1) and Vulcan 3 Graphite (V3G), respectively, with an aqueous solution of iron nitrate [Fe(NO<sub>3</sub>)<sub>3</sub> · 9H<sub>2</sub>O from Baker Chemical Co.]. The Carbolac-1 from Cabot Corporation has a total specific surface area of 950 m<sup>2</sup> g<sup>-1</sup> and the Vulcan 3 Graphite, obtained after graphitizing nonporous Vulcan 3 carbon black (from Cabot) at 3073 K, has a surface area of 56 m<sup>2</sup> g<sup>-1</sup>. For the C-1 catalyst, 2.5 cm<sup>3</sup> solution g<sup>-1</sup> was used while 1.0 cm<sup>3</sup> solution g<sup>-1</sup> was used for the V3G support. The solution was added dropwise and the catalyst was thoroughly stirred after each addition. One additional catalyst, 5% Fe/V3R, was prepared by heating the Vulcan 3 black in flowing H<sub>2</sub> for 12 hr at 1223 K to remove residual sulfur, then this carbon was impregnated in a similar manner. Without this S-removal step, the catalyst is inactive (6). Active iron/glassy carbon catalysts were also prepared by heating the glassy carbon (GC) prepared from paratoluene sulfonic acid in H<sub>2</sub> at 1223 K for 12 hr to remove sulfur prior to impregnation (6, 7). Saran (Dow Chemical Co.) was first carbonized in N<sub>2</sub> at 1223 K, then one sample was activated to 30% burnoff in CO<sub>2</sub> and

another was oxidized by treatment with  $\text{HNO}_3$  (6). The gases used, He (Matheson—99.9999% purity),  $\text{H}_2$  (Matheson—99.999% purity), and CO (Matheson—99.99% purity), were further purified (6).

CO and hydrogen uptakes were measured in a mercury-free, glass volumetric adsorption system which has been described elsewhere (8). All samples were reduced 16 hr in flowing  $\text{H}_2$  at 673 K followed by a 1 hr evacuation at 648 K before cooling under dynamic vacuum to the desired temperature. Isotherms were measured after a 1 hr exposure to the adsorbate.

Kinetic studies were conducted in a small glass reactor suspended in a fluidized sand-bath, which has been described elsewhere (6). Catalyst charges to the reactor were 1 g or less and conversions near 5% or lower were maintained to achieve operation of a differential, plug-flow reactor. Except for the activity maintenance studies, kinetic data were obtained after a 20-min period on-stream following a 20-min exposure to pure  $\text{H}_2$  (9). All samples, unless otherwise noted, were reduced 16 hr at 673 K in  $50 \text{ cm}^3 \text{ min}^{-1} \text{ H}_2$  before cooling in  $\text{H}_2$  to the desired temperature. Rates of CO hydrogena-

tion are based only on CO converted to hydrocarbons utilizing carbon balances on GC analyses (9).

After careful passivation in air, X-ray line broadening experiments were conducted using a Rigaku Geigerflex 4036-Al diffractometer, and average iron particle sizes were calculated using the Sherrer equation with Warren's correction for instrumental broadening.

Few studies have been reported which have examined the adsorption of CO and  $\text{H}_2$  on pure iron or on supported, unpromoted iron catalysts. The pioneering work of Emmett and co-workers was directed predominantly toward unsupported, singly, and doubly promoted iron catalysts (10). Recent UHV studies by Wedler *et al.* on iron films have clearly shown that both  $\text{H}_2$  and CO adsorb rapidly at 273 K and coverages which became essentially pressure-independent were attained by  $10^{-2} \text{ Pa}$  (11, 12). Thorough studies on MgO-supported iron have also shown that CO adsorbs readily on reduced iron surfaces, but activated  $\text{H}_2$  adsorption occurred on small iron crystallites ( $<15 \text{ nm}$ ) (13). Some uncertainty exists regarding characterization of iron by selective

TABLE I  
Iron Crystallite Sizes Determined by Chemisorption and X-Ray Diffraction Measurements

Catalyst	Uptake at 300 K ( $\mu\text{mole g catalyst}^{-1}$ )		Fe crystallite size (nm)	
	$\text{H}_2$	CO	$\text{CO}/\text{Fe}_s = \frac{1}{2}$	XRD <sup>b</sup>
Group "HD"				
4.8% Fe/Act. Saran	2.1	$>436^a$	$<0.7$	NV <sup>c</sup> ( $<4$ )
2.5% Fe/C-1	0.7	190	0.6	—
5.0% Fe/C-1	3.1	375	1.0	NV
5.9% Fe/Ox. Saran	7.1	$>241^a$	$<1.6$	NV
Group "LD"				
5.0% Fe/V3R	0.2	38	9	12
2.5% Fe/GC	0	3.9	43	26
4.5% Fe/V3G	1.3	5.6	54	33
5.0% Fe/Red. GC	0.7	4.0	83	21
10% Fe/ $\eta\text{-Al}_2\text{O}_3$	0	10.5	64	26

<sup>a</sup> Adsorption equilibrium had not been completely attained after 1 hr.

<sup>b</sup> Based on the (110)  $\alpha\text{-Fe}$  peak.

<sup>c</sup> Not visible.

TABLE 2  
Influence of Particle Size on Specific Activity<sup>a</sup>

Catalyst	Diameter (nm)	Activity ( $\mu\text{mol s}^{-1} \text{g Fe}^{-1}$ )		Turnover frequency ( $\text{s}^{-1} \times 10^3$ )	
		CH <sub>4</sub>	CO	N <sub>CH<sub>4</sub></sub>	N <sub>CO</sub>
4.8% Fe/Act. Saran	<0.7	11	51	1.2	5.7
2.5% Fe/C-1	0.6	12	58	1.5	7.9
5.0% Fe/C-1	1.0	18	69	2.5	9.3
5.9% Fe/Ox. Saran	<1.6	20	72	5.0	18
5.0% Fe/V3R	9.0	9.4	37	12	50
2.5% Fe/GC	43	6.0	26	38	167
4.5% Fe/V3G	54	13	69	107	554
5.0% Fe/Red. GC	83	2.6	11	33	138
10% Fe/Al <sub>2</sub> O <sub>3</sub>	64	6.1	16	58	152

<sup>a</sup>  $P = 101 \text{ kPa}$ ,  $T = 548 \text{ K}$ ,  $\text{H}_2/\text{CO} = 3$ .

gas chemisorption (14), and the adsorption stoichiometry of CO ( $\text{Fe}_s : \text{CO}$ ) might be expected to vary between 1 and 2 (15); however, good agreement among different techniques to measure particle size has been obtained assuming a ratio of 2:1 (15). Regardless, CO chemisorption at 300 K should be a good *relative* measure of iron surface area and provide absolute surface areas accurate to within a factor of two. Turnover frequencies were calculated here based on these values for fresh catalysts and assuming an adsorption stoichiometry of  $\text{Fe}_s/\text{CO} = 1$ . Adsorption blanks were run on the pure carbon supports and no irreversible adsorption occurred at any temperature (16). A slow CO uptake continued after 1 hr on the two Saran-supported catalysts, and it is not known at this time whether adsorption on the carbon support or on the iron surface was occurring. All uptakes in Table 1 are those measured after a 1-hr exposure to CO. The CO chemisorption results in Table 1 clearly show that small iron particles are present in the high dispersion (HD) family of catalysts, and large iron particles exist in the low dispersion (LD) group, regardless of choice of adsorption stoichiometry.

Average particle sizes,  $d$ , were calculated using CO uptakes and the equation  $d(\text{nm}) =$

$C/D$  with  $C = 0.75 \text{ nm}$  and  $D = \text{Fe}_s/\text{Fe}_t$  where  $\text{Fe}_s$  represents surface Fe atoms and  $\text{Fe}_t$  is the total number of Fe atoms. The value of  $C$  is obtained using an average area per  $\text{Fe}_s$  atom of  $9.4 \text{ \AA}^2$  (10). Table 1 shows that CO uptakes on the HD catalysts are very large compared to uptake on the LD samples. The hydrogen chemisorption values at 300 K are consistently low, and although such behavior has been reported previously (9, 17), it is not well understood at this time. Activated hydrogen chemisorption over this temperature range has recently been reported on small iron particles (13), but this does not explain the low  $\text{H}_{(\text{a})}/\text{CO}_{(\text{a})}$  ratios on the large, carbon-supported iron crystallites.

X-Ray diffraction results were generally in qualitative agreement with the chemisorption results, assuming bridged bonding, as shown in Table 1. The HD catalysts showed no visible Fe peaks because they were so broad, whereas all the LD catalysts exhibited well-defined diffraction peaks. Characterization in much greater detail using CO chemisorption at 195 K, magnetic susceptibility measurements, and Mössbauer spectroscopy has clearly shown that small iron crystallites were present in the 5.0% Fe/C-1 catalyst while large iron crys-

TABLE 3  
KINETIC PARAMETERS FOR Fe/CARBON CATALYSTS<sup>a</sup>

Catalyst	A ( $\frac{\text{molecules}}{\text{site} \cdot \text{s} \cdot \text{ATM}}$ )	E <sub>CH<sub>4</sub></sub> (kJ/mole)	X	Y	E <sub>CO</sub> <sup>b</sup> (kJ/mole)
4.8% Fe/Act. Saran	$2.35 \times 10^4$	76	1.15	-0.17	67
2.5% Fe/C-1	—	82	—	—	84
5.0% Fe/C-1	$1.81 \times 10^6$	93	1.04	-0.14	87
5.9% Fe/Ox. Saran	$2.09 \times 10^6$	90	1.08	-0.07	75
5.0% Fe/V3R	$4.07 \times 10^6$	88	0.98	-0.01	95
2.5% Fe/GC	$5.48 \times 10^8$	107	0.96	-0.26	133
4.5% Fe/V3G	$1.06 \times 10^8$	93	1.49	-0.13	105
5.0% Fe/Red. GC	—	105	—	—	122
10% Fe/Al <sub>2</sub> O <sub>3</sub>	—	72	—	—	64
15% Fe/Al <sub>2</sub> O <sub>3</sub> <sup>c</sup>	$2.28 \times 10^7$	89	1.14	-0.05	109

$$^a N_{\text{CH}_4} = A e^{-E/RT} P_{\text{H}_2}^x P_{\text{CO}}^y$$

<sup>b</sup> CO conversion to hydrocarbons.

<sup>c</sup> From Ref. (9).

tallites existed in the 4.5% Fe/V3G sample, and these results are reported elsewhere (16, 18).

An important consequence of this study is the capability of preparing very small supported iron crystallites because iron is a metal difficult to prepare in such a state. MgO-supported iron is the only other highly

dispersed iron system that has been reported (13, 15), but two additional advantages are obtained by the use of carbon supports—they are very inert and essentially all of the iron can be reduced to metallic iron (18).

These carbon-supported iron catalysts are very active as shown in Table 2. These

TABLE 4  
Product Distributions from Carbon-Supported Iron<sup>a</sup>

Catalyst	T (°K)	CO conv. (%)	Mole fraction						Olefin/paraffin ratio <sup>b</sup>
			C <sub>1</sub>	C <sub>2</sub>	C <sub>3</sub>	C <sub>4</sub>	C <sub>5</sub>	C <sub>6+</sub>	
4.8% Fe/Act. Saran	503	3.1	40	30	20	7	3	2	1.8
2.5% Fe/C-1	523	3.2	43	23	16	11	5	3	1.5
5.0% Fe/C-1	503	3.0	49	19	18	9	3	2	1.2
5.9% Fe/Ox. Saran	499	3.6	46	18	15	9	7	5	1.7
5.0% Fe/V3R	528	2.8	54	18	16	7	3	2	1.3
2.5% Fe/GC	528	3.2	55	19	18	6	3	Tr	0.35
4.5% Fe/V3G	518	3.9	48	16	18	9	6	4	0.53
5.0% Fe/Red. GC	528	3.0	52	21	18	7	2	Tr	0.23
10% Fe/Al <sub>2</sub> O <sub>3</sub>	499	3.4	58	14	17	8	2	1	0.65
10% Fe/Al <sub>2</sub> O <sub>3</sub>	504	4.7	59	14	16	8	2	1	0.20

<sup>a</sup> P = 101 kPa, H<sub>2</sub>/CO = 3.

<sup>b</sup> C<sub>2</sub> + C<sub>3</sub>.

activities are orders of magnitude higher than those calculated for other iron/carbon systems (19, 20), and all are comparable to or higher than those for Fe/Al<sub>2</sub>O<sub>3</sub> catalysts on a gram Fe basis. On a turnover frequency (TOF) basis, only the low dispersion (LD) Fe/carbon catalysts had values similar to the Fe/Al<sub>2</sub>O<sub>3</sub> catalyst, as shown in Table 2. An obvious conclusion from Table 2 is that TOF values ( $N_{\text{CH}_4}$  or  $N_{\text{CO}}$ ) are lower on small iron crystallites than on large crystallites. A clear trend exists and the TOF increases smoothly more than 20-fold as iron crystallite size increases from about 10 to over 400 Å. The HD catalysts, with average particle sizes below 30 Å, have  $N_{\text{CO}}$  values at 548 K usually below 0.01 s<sup>-1</sup> and  $N_{\text{CH}_4}$  values near 0.001 s<sup>-1</sup> whereas  $N_{\text{CH}_4}$  values are higher than 0.03 s<sup>-1</sup> and  $N_{\text{CO}}$  values increase to 0.14 or higher on large iron crystallites. This trend is in agreement with that reported by Storm and Boudart for methanation over MgO-supported iron (21). As indicated in Table 2, on a gram iron or gram catalyst basis, activities of all carbon-supported iron catalysts are similar because the lower TOFs on HD catalysts are compensated for by the higher iron surface areas. It is important to point out that the lower TOF values on small Fe particles eliminates the possibility that particle heating due to the exothermicity of the reaction is causing this effect. Kinetic parameters for methanation are shown in Table 3. Partial pressure dependencies were typically near first order in H<sub>2</sub> and zero order in CO. The lower TOFs on small Fe crystallites cannot be attributed to higher activation energies. Over the carbon-supported iron catalysts a marked increase occurred in the olefin/paraffin ratio, which was especially pronounced for the HD group and was nearly 10-fold greater than the ratio for the Fe/Al<sub>2</sub>O<sub>3</sub> catalysts (5, 16). Table 4 shows these results which were obtained at nearly identical CO conversions because this parameter can have a much greater effect on this ratio than a

small variation in temperature (22). The two values for the 10% Fe/Al<sub>2</sub>O<sub>3</sub> substantiate the sensitivity to conversion. Some of the HD catalysts exhibited ratios that were surprisingly insensitive to conversion, and values near two persisted at conversions over 5% (16). In addition to a greater capability to produce olefins, the HD catalysts showed a lower methane make, as also indicated in Table 4.

Excellent activity maintenance represented another improvement in catalytic behavior exhibited by the HD iron/carbon catalysts. Methanation activity was constant over the 5% Fe/C-1 catalyst during 45 hr of continuous operation on-stream at 101 kPa as shown in Fig. 1. Overall CO conversion decreased slightly during the first hour or two on-stream then it too remained stable within experimental error. Such behavior is unusual for iron catalysts, as slow deactivation processes normally set in after a certain period on-stream (17, 23), and this expected behavior was exhibited by the 10% Fe/Al<sub>2</sub>O<sub>3</sub> and 4.5% Fe/V3G catalysts, both of which contained large iron crystallites. These HD catalysts do not sinter readily and CO uptakes are still very large on used samples taken from the reactor (6, 16). Product distributions were constant during this 45-hr period.

The lower turnover frequencies, decreased selectivities to methane, and the higher olefin/paraffin ratios exhibited by the HD iron/carbon catalysts are consistent with the proposal that surface coverage of hydrogen under reaction conditions is much lower on small iron crystallites. The marked inhibition of hydrogen chemisorption at temperatures up to 473 K found by Tøpsøe *et al.* for small iron crystallites strongly supports this conclusion (13). The first order pressure dependence of CO hydrogenation on hydrogen predicts that a decrease in the surface concentration of hydrogen would proportionally decrease specific activity. This model does not readily explain the superior activity mainte-

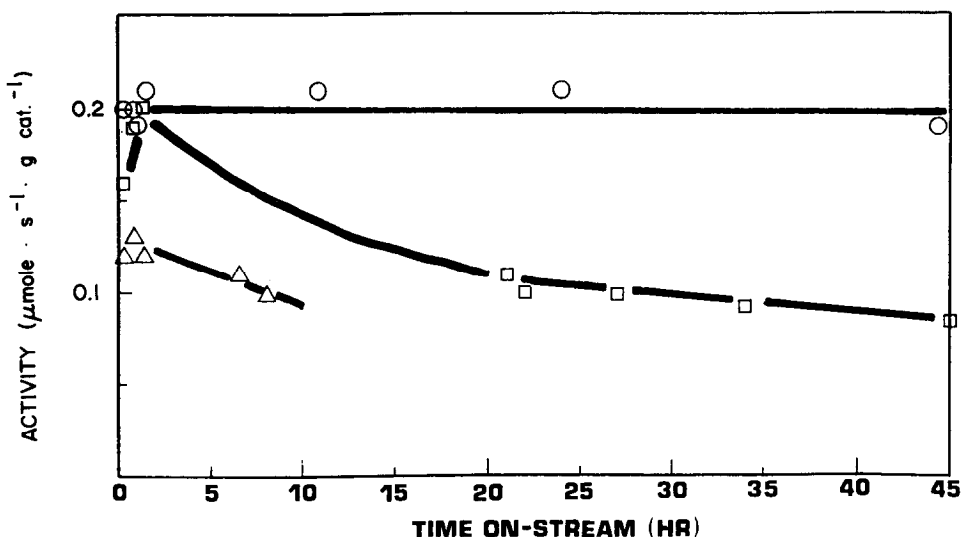


FIG. 1. Rate of  $\text{CH}_4$  formation as a function of time on-stream.  $P = 101$  kPa,  $T = 508$  K,  $\text{H}_2/\text{CO} = 3$ ;  $\circ$ , 5.0% Fe/C-1;  $\triangle$ , 4.5% Fe/V3G;  $\square$ , 10% Fe/ $\text{Al}_2\text{O}_3$ .

nance of these HD catalysts, however, and this property may be a consequence of the rapid formation and stabilization of active iron carbide phases (17, 18, 24). The presence of very small iron crystallites facilitates rapid carbide formation, and future work is required to determine if the carbon support plays a role in stabilizing these carbide phases after their formation.

#### ACKNOWLEDGMENTS

This research was supported by NSF Grant ENG 76-82099, and NSF Grant CPE-7915761. The latter Grant is cosponsored by the U.S. Army Research Office.

#### REFERENCES

- Vannice, M. A., *Cat. Rev.-Sci. Eng.* **14**, 153 (1976).
- Vannice, M. A., and Garten, R. L., *J. Catal.* **63**, 255 (1980).
- Aika, K., Hori, H., and Ozaki, A., *J. Catal.* **27**, 424 (1972).
- Schmitt, J. L., and Walker, P. L., *Carbon* **9**, 791 (1971); *Carbon* **10**, 87 (1972).
- Moreno-Castilla, C., Mahajan, O. P., Jung, H.-J., Vannice, M. A., Walker, P. L., Jr., Absts. 14th Amer. Carbon Conf., Penn State U., June, 1979.
- Vannice, M. A., Walker, P. L., Jung, H.-J., Moreno-Castilla, C., and Mahajan, O. P., *Proc. VII Int. Cong. Catal. Tokyo*, Paper A31, July (1980).
- Moreno-Castilla, C., Mahajan, O. P., Walker, P. L., Jr., Jung, H.-J., and Vannice, M. A., *Carbon* **18**, 271 (1980).
- Palmer, M. B., and Vannice, M. A., *J. Chem. Tech. Biotechnol.* **30**, 205 (1980).
- Vannice, M. A., *J. Catal.* **37**, 449 (1975).
- Emmett, P. H., and Takezawa, N., *J. Res. Inst. Catal., Hokkaido Univ.* **26-1**, 37 (1978).
- Wedler, G., Geuss, K. P., Colb, K. G., and McElhiney, G., *Appl. Surf. Sci.* **1**, 471 (1978).
- Wedler, G., Colb, K. G., McElhiney, G., and Heinrich, W., *Appl. Surf. Sci.* **2**, 30 (1978).
- Tøpsøe, H., Tøpsøe, N., Bohlbro, H., and Dumesic, J. A., *Proc. 7th Int. Cong. Catal.* A15 (1980).
- Farrauto, R. J., *AIChE Symp. Ser.* **143** **70**, 9 (1974).
- Boudart, M., Delbouille, A., Dumesic, J. A., Khammouma, S., and Tøpsøe, H., *J. Catal.* **37**, 486 (1975).
- Jung, H.-J., Ph.D. Thesis, Pennsylvania State Univ. (1981).
- Raupp, G. B., and Delgass, W. N., *J. Catal.* **58**, 361 (1979).
- Jung, H.-J., Mulay, L. N., Vannice, M. A., Stanfield, R. M., and Delgass, W. N., *J. Catal.*, in press.

19. Kikuchi, E., Ino, T., Ito, N., and Morita, Y., *Bull. Japan. Petr. Inst.* **18**, 139 (1976).
20. Parkash, S., and Chakrabartty, *Carbon* **16**, 231 (1978).
21. Storm, D., and Boudart, M., *Abst. 6th N. Amer. Catal. Soc. Meeting, Chicago, March, 1979*.
22. Ott, G. L., Fleisch, T., and Delgass, W. N., *J. Catal.* **65**, 253 (1980).
23. Dwyer, D. J., and Somorjai, G. A., *J. Catal.* **52**, 291 (1978).
24. Amelse, J. A., Butt, J. B., and Schwartz, L. H., *J. Phys. Chem.* **82**, 558 (1978).

H-J. JUNG<sup>1</sup>  
P. L. WALKER, JR.<sup>2</sup>  
M. ALBERT VANNICE<sup>1</sup>

<sup>1</sup> *Department of Chemical Engineering*

<sup>2</sup> *Department of Materials Science and Engineering  
The Pennsylvania State University  
University Park, Pennsylvania 16802*

*Received July 21, 1981; revised November 2, 1981*